ICT - Information and Communication Technologies

Merging Plasmonic and Silicon Photonics Technology towards Tb/s routing in optical interconnects

Collaborative Project

Grant Agreement Number 249135

D4.3: Fabrication, characterization and system-level evaluation of a 4x4 thermooptic DLSPP-based switching matrix

Due Date of Deliverable: 31/03/2012

Actual Submission Date: 22/05/2012

Revision: Draft

Start date of project: January 1st 2010 **Duration:** 36 months

Organization name of lead contractor for this deliverable: SDU

Author: **F. Zacharatos (UB)**

Contributors: K. Hassan (UB), L. Markey (UB), J.C. Weeber (UB), A.Dereux (UB), M. Waldow (AMO), A. Kumar (SDU), V.S. Volkov (SDU), J. Gosciniak (SDU), S.I. Bozhevolnyi (SDU), O. Tsilipakos (CERTH/ITI) A. Pitilakis (CERTH/ITI), E. Kriezis (CERTH/ITI), K. Vyrsokinos (CERTH/ITI), G. Kalfas (CERTH/ITI), S. Papaioannou (CERTH/ITI), N. Pleros (CERTH/ITI), D. Kalavrouziotis (ICCS/NTUA), G. Giannoulis (ICCS/NTUA), D. Apostolopoulos (ICCS/NTUA), H. Avramopoulos (ICCS/NTUA)

Project Information

PROJECT	
Project name:	Merging Plasmonic and Silicon Photonics Technology towards Tb/s routing in optical interconnects
Project acronym:	PLATON
Project start date:	01/01/2010
Project duration:	36 months
Contract number:	249135
Project coordinator:	Nikos Pleros – CERTH
Instrument:	STREP
Activity:	THEME CHALLENGE 3: Components, Systems, Engineering

DOCUMENT	
Document title:	Fabrication and performance evaluation of the WRR 2x2 DLSPP switch
Document type:	Report
Deliverable number:	D4.3
Contractual date of delivery:	31/03/2012
Calendar date of delivery:	22/05/2012
Editor:	F. Zacharatos (UB)
Authors:	M. Wildow, A. Kumar, V.S. Volkov, J. Gosciniak, S.I. Bozhevolnyi, K. Hassan, L. Markey, J.C. Weeber, A.Dereux, K. Vyrsokinos, S. Papaioannou, N. Pleros, D. Kalavrouziotis,G. Giannoulis, D. Apostolopoulos, H. Avramopoulos, F. Zacharatos
Workpackage number:	WP4
Workpackage title:	Development and system-evaluation of plasmonic switching elements
Lead partner:	SDU
Dissemination level:	CO
Date created:	31/03/2012
Updated:	
Version:	v1
Total number of Pages:	17
Document status:	final

TABLE OF CONTENTS

1 EXECUTIVE SUMMARY 4

2 INTRODUCTION 5

3 DESIGN OF THE 4X4 CYCLOMER DLSPP SWITCHES 6

3.1 SWITCHING MATRIX COMPOSED FROM A-MZIS 6

3.2 DWRR SWITCHING MATRIX 7

4 EXPERIMENTAL EVALUATION OF PMMA- AND CYCLOMER- LOADED SOI-DLSPP WRR SWITCHES 8

4.1 SOI PLATFORM PROCESSING BY AMO 8

4.2 PLASMONIC WAVEGUIDE FABRICATION BY UB 9

5 EXPERIMENTAL EVALUATION OF CYCLOMER- LOADED SPP BASED THERMOOPTIC 4X4 SWITCHING MATRIX 12

5.1 STRUCTURAL CHARACTERIZATION OF SOI-TO-DLSPP AMZI 4X4 SWITCHES 12

5.2 ELECTRICAL-OPTICAL CHARACTERIZATION 13

5.3 CHARACTERIZATION OF A 4X4 THERMOOPTIC DUAL RING RESONATOR CYCLOMER LOADED SPP SWITCHING MATRIX 14

6 CONCLUSIONS 16

ABBREVIATIONS 17

1 Executive Summary

This document provides a detailed analysis of the design, fabrication and the first experimental results obtained from 4x4 switching matrices that will be adopted in the final 4x4 PLATON router.

Two different cells of 4x4 DLSPP based A-MZI switching matrix designs have been included in the latest (3rd) PLATON Mask design for SOI integration by UV lithography. The first one was based on a symmetric MZI with 40μm length phase arms and the second an A-MZI with 20μm length arms. The A-MZI structures have been fabricated by employing a novel bi-layer lithographic process that leads to optimized structural characteristics at the Gold level. Furthermore, an investigation towards the optimal UV dose for the Cyclomer level lithography brought about interesting results that will be described in detail in the following paragraphs.

Moreover, a 4x4 thermo-optic DLSPP switching device relying on four X-add-drop structures linked together in a 4x4 non blocking switch configuration has been tested with fast prototyping process. Light propagation in this 4x4 switching device has been observed by Leakage Radiation Microscopy (LRM) demonstrating successful routing of the incoming signal. The 4x4 system was investigated in terms of operation by employing two different wavelengths spaced by ≈25nm, revealing clear switching of direction between the two output ports. Further evaluation of the switching matrix with true data signals was not possible due to excessive losses of the chip that were >60dB. Currently the chips are under evaluation for the identification of the high losses.

2 Introduction

According to the work plan, this deliverable is related to WP4 objectives summarized as:

To develop and evaluate in a single fabrication step a 4x4 DLSPP-based switching matrix composed by:

i. Symmetric -MZIs with 40μm length phase arms as switching elements

ii. Asymmetric-MZIs with 20μm length phase arms as switching elements

iii. dual X-add/drop ring/racetrack resonators in cross configuration as switching elements without crosspoint treatment

iv. dual X-add/drop ring/racetrack resonators in cross configuration as switching elements with crosspoint treatment

The evaluation of the 4x4 switches composed with dual X-add/drop ring/racetrack resonators has been performed under static conditions by varying the wavelength of the incoming signals and detection of the output ports with LRM. The evaluation of the 4x4 switches with MZI as switching elements has revealed excessive losses (>60dB) that prohibited their operation with true data traffic. Further investigation is currently under way for the identification of the excessive losses of the chip.

This deliverable is associated with Task 4.3 "Fabrication, characterization and system-level evaluation of a 4x4 thermooptic DLSPP-based switching matrix" [M21-M27].

The successful development and evaluation of the 4x4 DLSPP-based switching elements is considered as an important step towards the deployment and the performance optimization of the complete 4x4 router prototype.

3 Design of the 4x4 Cyclomer DLSPP switches

3.1 Switching matrix composed from A-MZIs

Two different 4x4 switching matrices composed from A-MZIs are located in the second die of the 3rd design PLATON UV mask. In this mask, the Si and DLSPP waveguide dimensions are identical to PLATON waveguide specifications that have been used so far. Also the DLSPP waveguides use Cyclomer as the dielectric polymer and the TM grating couplers for coupling light in and out of the chip follow the fully etched design proposed recently by IZM with ~3.25dB experimental losses. However no Spin on Glass has been deposited on top of the Grating Couplers, presumably affecting their performance. For monitoring purposes 90:10 couplers are placed on the layout with 90% port goes to the 4x4 switch, while 10% port is connected to a grating coupler. The specifications of the structures included in the 3rd mask design can be found in D1.4. In this document the A-MZI switching elements' design including two different 4x4 matrices is reported:

a) hybrid Si-DLSPP 4x4 symmetric MZI switch using 40μm-long MZI arms

b) hybrid Si-DLSPP 4x4 asymmetric MZI (A-MZI) switch using 20μm-long MZI arms with one of them being 313nm longer in order to achieve the differential biasing

The following images correspond to the structures comprising the two matrices and have been copied from the original GDS mask design file.

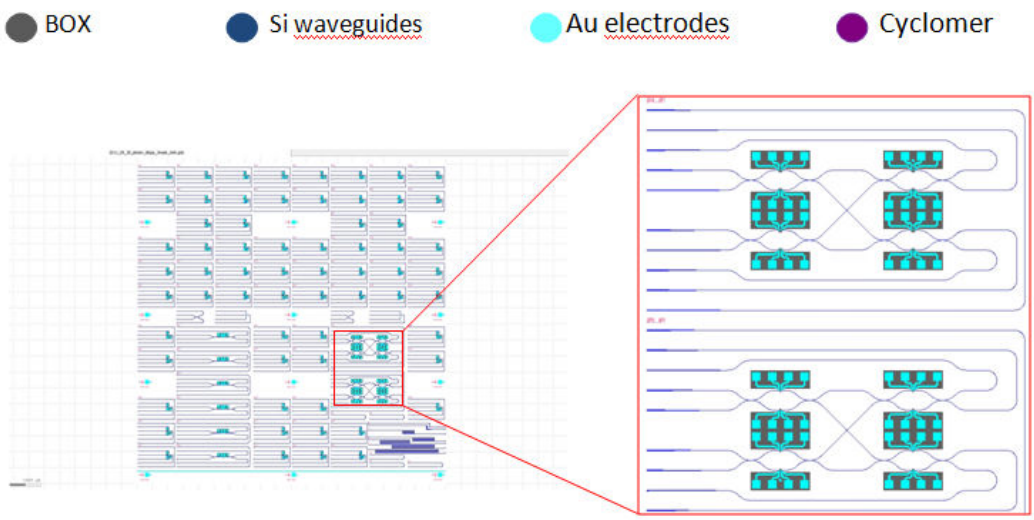

Figure 3.1 Overview of the 3rd design Platon mask and zoom in at the 4x4 MZI die

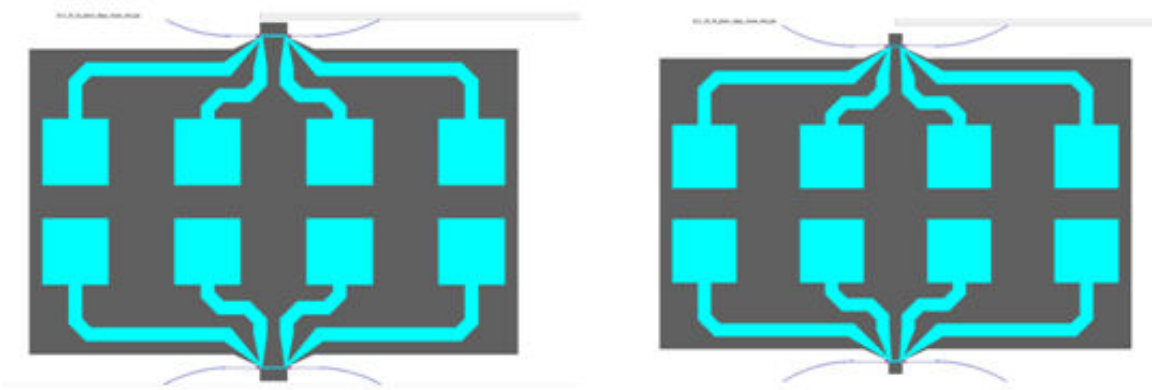

Figure 3.2. Cells comprised of 2 MZI's. Left: 40μm arms. Right:20μm arms

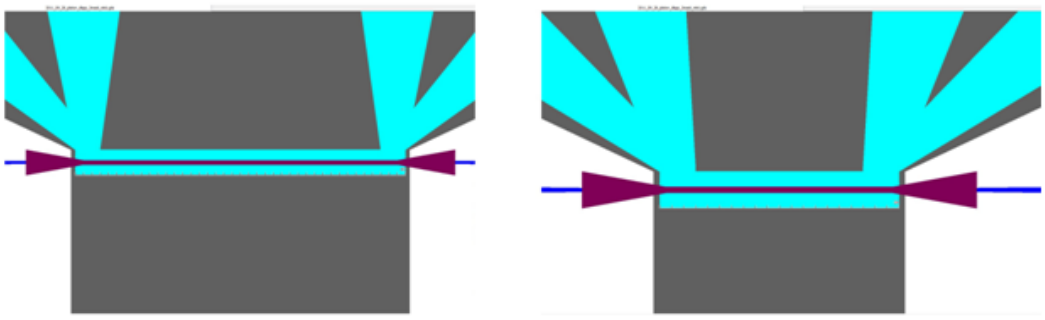

Figure 3.3. Closer look at the Cyclomer loaded arms. Left: 40μm arms. Right:20μm arms

3.2 DWRR switching matrix

A 4x4 dual waveguide ring resonator switching matrix is also reported in this document. This specific switch relied on four X-add-drop structures linked together (Figure 3.4), following the design predicted by simulations performed by CERTH.

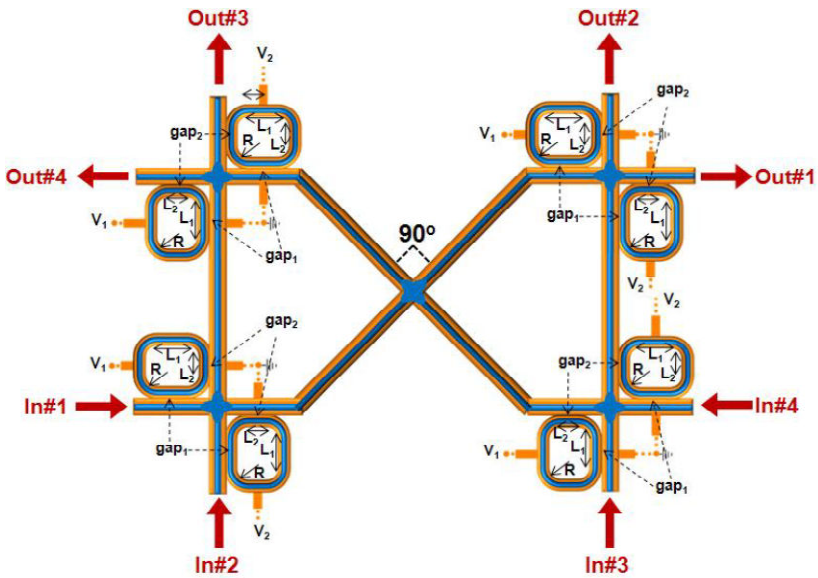

Figure 3.4: Schematic layout of a 4x4 thermo-optic DLSPP-based switch

4 Experimental evaluation of PMMA- and Cyclomer- loaded SOI-DLSPP WRR switches

The fabrication process for the hybrid Si-DLSPPW 4x4 switching structures has been divided into two basic building blocks: a) the SOI fabrication platform provided by AMO and b) the subsequent fabrication of the plasmonic waveguides by UB.

4.1 SOI platform processing by AMO

Processing is based on standard 6" SOI wafers with a top silicon thickness of 340 nm and a buried oxide layer of 2 µm. For the realization of the SOI platform a mix & match lithography approach has been chosen by AMO, combining flexible high resolution electron beam lithography (EBL) with fast optical lithography utilizing an i—Line stepper tool. In a first process module, a marker layer providing alignment markers for all subsequent process steps has been defined using optical lithography and transferred into the substrate wafer using a dedicated reactive ion etching (RIE) process. After removal of residual resist and cleaning of the wafers the silicon waveguide structures have been defined by EBL using HSQ as negative tone resist material. A multi-pass grey scale exposure technique has been applied which provides both excellent CD control (especially needed for high quality grating coupler structures featuring constant coupling efficiencies) and low loss waveguides. To improve the overlay accuracy with the subsequent plasmonic process steps and therefore increase the overall yield of the fabrication process the initial design had been divided into four quadrants which were exposed separately on different dies. Due to the combination of flexible EBL and fast optical lithography the increased number of fabricated dies did not lead to a significant delay for the fabrication, as the flexibility of the EBL process allowed the definition of those different dies in only one lithography while at the same time the exposure time per die for the optical lithography is marginal compared with wafer handling times.

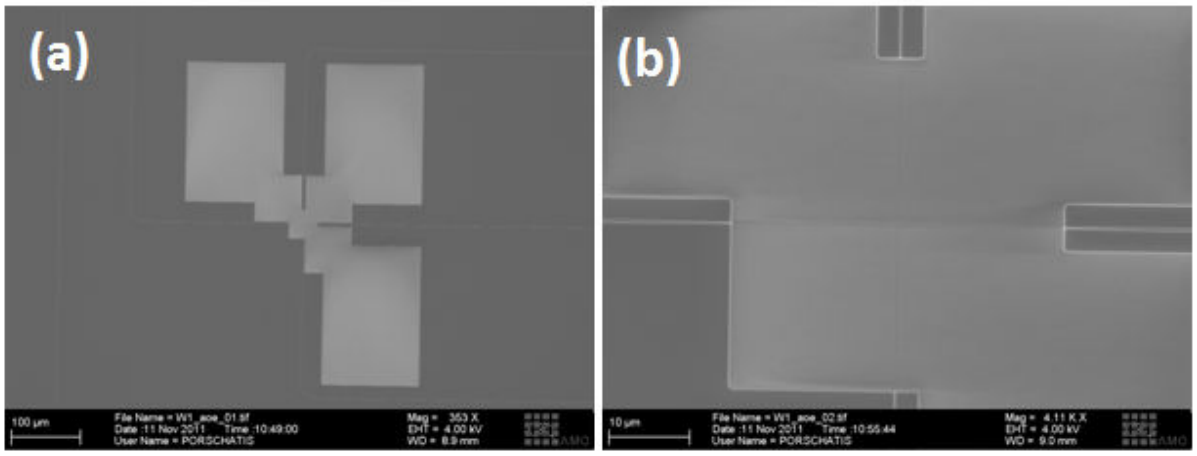

Figure 4.1: Exemplary SOI platform for DWRR device : a) device overview and b) side detailed view of etched cavity

Again, a dedicated RIE process has been used to transfer the resist mask 290 nm deep into the top silicon layer, resulting in rib waveguide structures with a slab height of 50 nm. The residual HSQ and passivation layers grown during the RIE processing have been removed by wet chemical processing.

In a final process module the SOI platform has been finalized by defining a resist mask for the coupling regions, again using optical lithography as a fast and high throughput

technology. This mask has then been used to remove the waveguide structures and the 50 nm silicon slab and to etch a 180 nm deep cavity into the buried oxide.

The resulting SOI building blocks for two exemplary devices are presented in the SEM micrographs in Figure 4.1**Error! Reference source not found.** and Figure 4.2. The so-fabricated SOI structures were then transferred to UB for further processing.

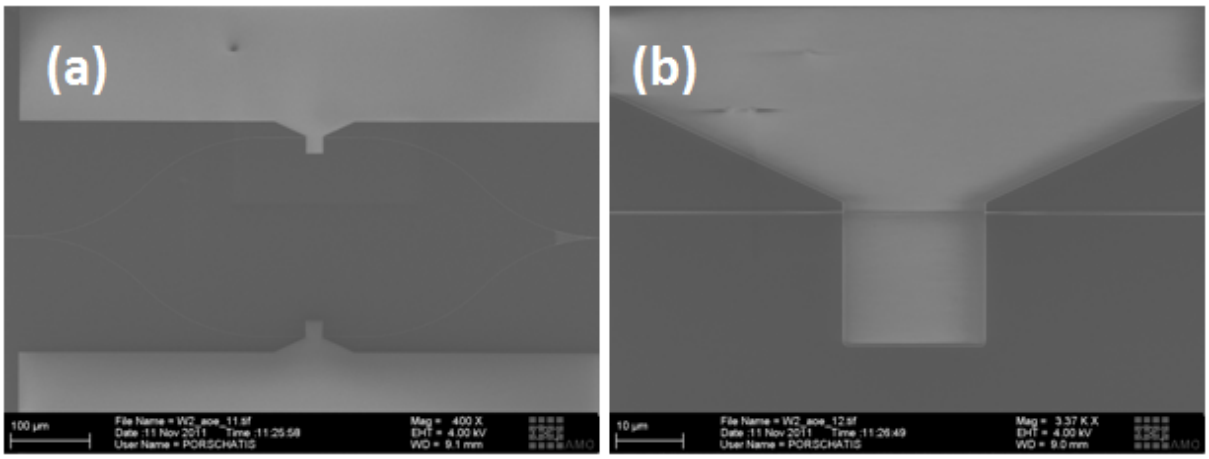

Figure 4.2: Exemplary SOI platform for 4x4 A-MZI device : a) device overview and b) detailed view of etched cavity

4.2 Plasmonic waveguide fabrication by UB

As described in section *3.1* the 3rd design mask includes among other structures one die with two 4x4 MZIs. The plasmonic part of the 4x4 MZI Gold electrodes & Cyclomer load has been processed by UB. A reliable process has been developed for the fabrication of the circuits with high reproducibility. The gold level fabrication has been optimized with respect to older mask designs by adopting a bi-layer lift-off resist process which will be explained in detail in the following paragraph. For the Cyclomer level it was adopted the UV250 lithography strategy that was described in detail in D3.1 section 6.1.3 and succeeded in improving the resolution of the waveguides by optimizing the UV dose.

Bi layer Photo Resist Process On SOI for Au Lift-off

Instead of using a single photoresist layer (AZnLOF) as in previous chips, this time a lift-off resist with commercial name LOR (provided by Microchem) was spin-coated on the SOI substrate before the actual imaging resist spin-coat. Used beneath photoresists in a bi-layer stack, LOR can extend the limits of lift-off processing beyond where single layer resist strategies can reach. LOR is not imaged during the exposure but is developed during the development step and improves the overall efficiency of the lift-off procedure. The process flow is described below:

1. Spin – coat LOR 07A:20A / 3:1 @3,000rpm for 40s
2. Soft bake @195° C for 3min
3. Spin – Coat AZnLOF 1:04 (AZ:EBR) @ 3,000 rpm for 40s
4. Soft bake @110° C for 3min
5. EBR 10 sec
6. UV 365nm exposure; dose: 46mJ
7. Post exposure bake @112° C for 4 min
8. Development with AZ826 MIF for 2min max, rinse with DI water
9. Flood exposure; dose: 370mJ

10. Hard bake @110° for 3 min
11. Evaporate metal
12. Lift-off in NMP @ 90° C for 1h max

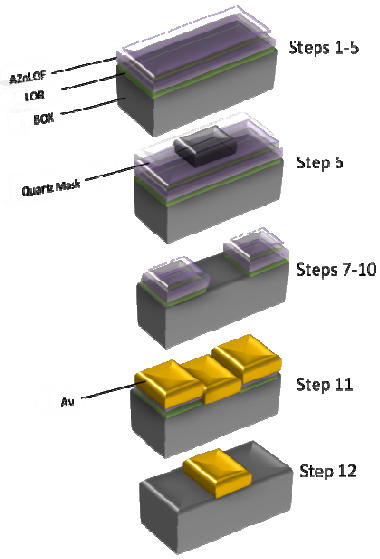

Figure 4.3: Process flow for the fabrication of the plasmonic waveguides

The main advantages of the novel lift-off process are:

- Lower Line Edge Roughness and sharper edges compared to the single layer (AZnLOF) process.
- Very short (10min) and efficient lift-off without any use of ultrasounds.

Figure 4.4 illustrates the two different resist layers as seen by focusing the optical microscope on the AZnLOF plane.

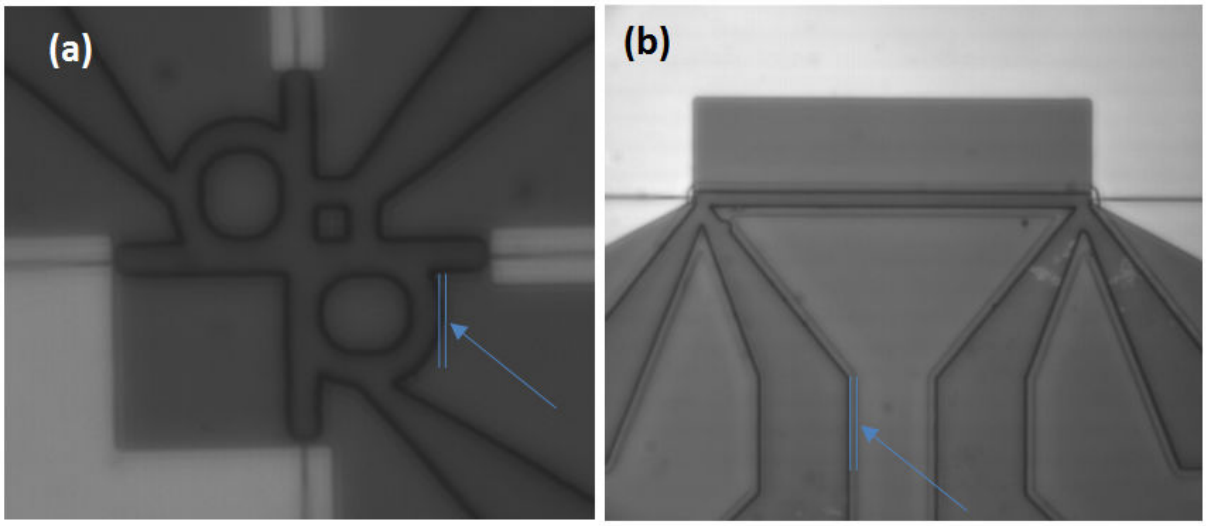

Figure 4.4: Optical micrographs of structures obtained after step 8 of the bi-layer photoresist process. The underlying (LOR) layer is marked. a) DWRR and b) MZI

Cyclomer Level Processing

For the Cyclomer Level the process mentioned in D1.4 was employed, however a UV dose of 750mJ instead of 800mJ was applied. This specific value is an outcome of a series of

investigation tests aiming at the dose factor optimization and resulted in lower LER and thus higher resolution with respect to previously processed chips. The following SEM images are representative of the improved result (after optimizing the dose factor) for the case of dual ring resonator gaps, which is the most demanding structure in terms of resolution.

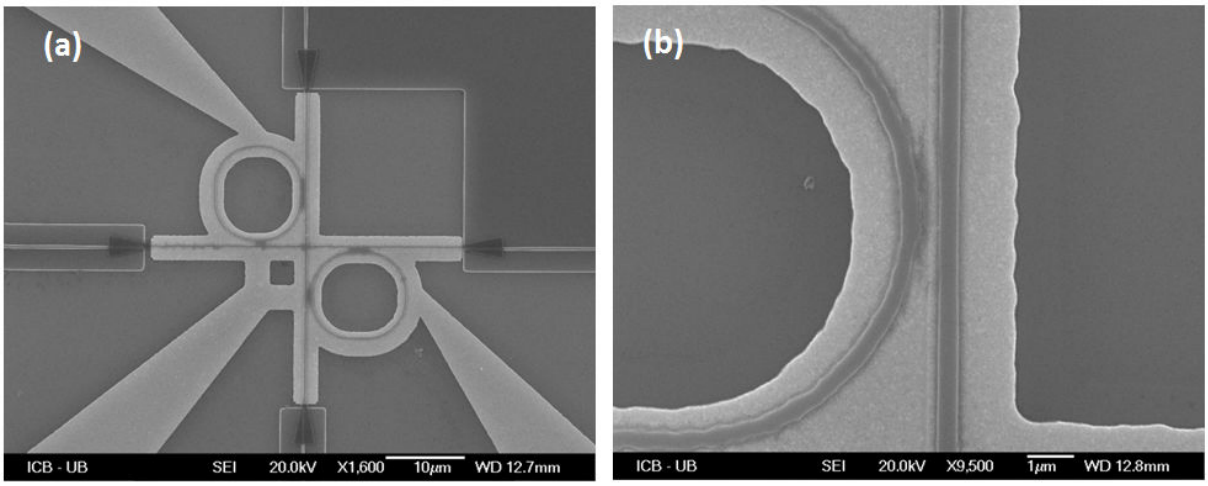

Figure 4.5: a) SEM micrograph of DWRR loaded with Cyclomer and b) closer look at the open gap. Gaps (350nm wide) are opened. Line Edges are smooth.

5 Experimental evaluation of Cyclomer- loaded SPP based Thermooptic 4x4 switching matrix

5.1 Structural Characterization of SOI-to-DLSPP AMZI 4x4 switches

The 4x4 die was characterized before shipment to SDU for characterization by SEM. The images below corresponds to the resulting 4x4 matrix.

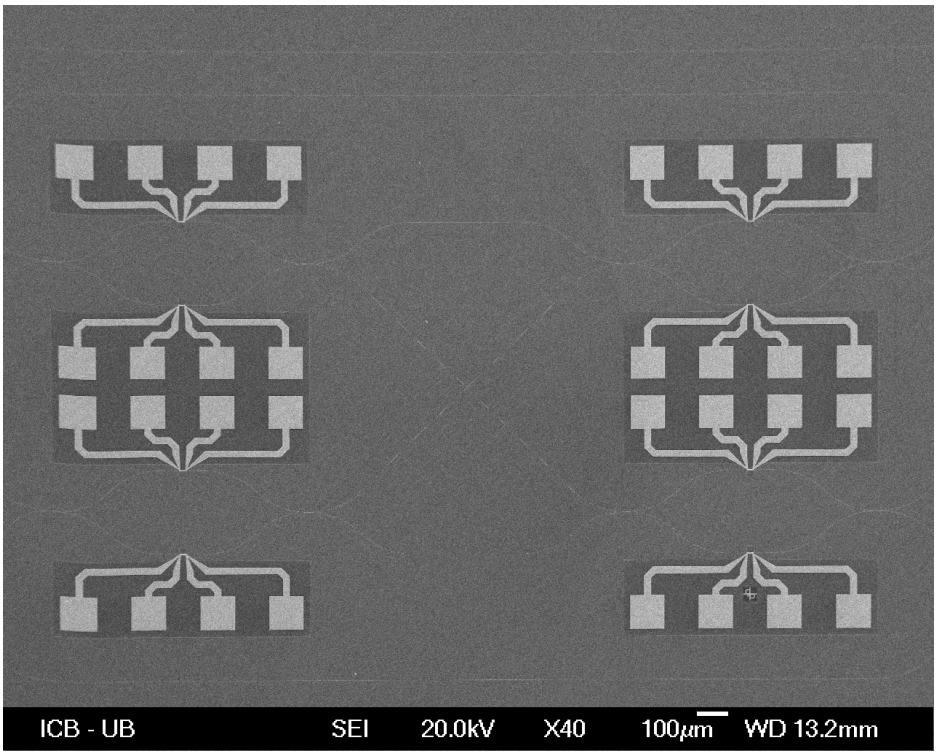

Figure 5.1: SEM micrograph of the first 4x4 A-MZI cell. The Au electrodes of each structure end up at 20μm arms loaded with Cyclomer straight or bent waveguides.

Below some SEM micrographs of MZI components are presented.

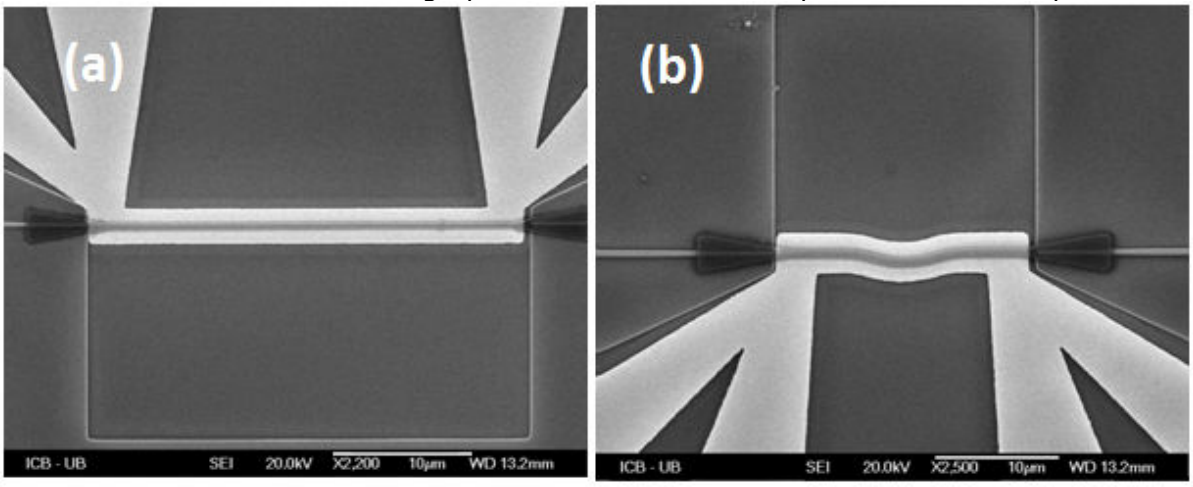

Figure 5.2: MZI arms closer look. a) SEM micrograph of straight 20μm long arm and b) SEM micrograph of bent 20μm long arm.

During the SEM characterization the geometrical characteristics of the MZIs were measured so as to be evaluated with respect to the nominal (by design) values.

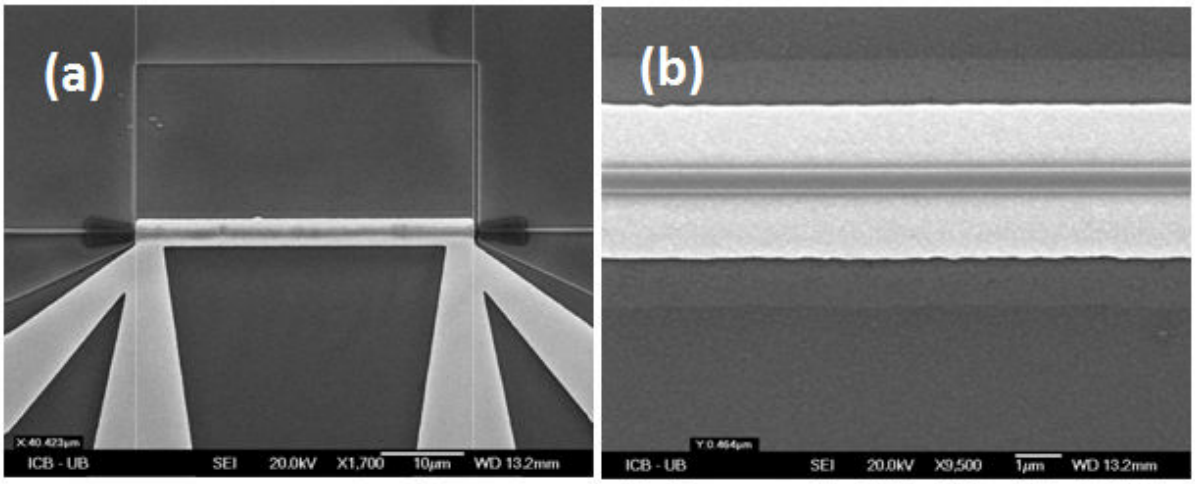

Figure 5.3: SEM measurements of Cyclomer loads dimensions. a) waveguide length (40.423 μm) and b) waveguide width (464nm).

The following Table 1 summarizes the structural characteristics of the 4x4 MZI structure by design and by fabrication. AFM characterization was employed in order to define the vertical dimensions of the fabricated structures.

Table 1: Comparison between designed and resulting MZI structural characteristics

Feature	Nominal	Actual	Variation %
Arms length (μm)	40 or 20	40±0.4 or 20±0.2	≈1
Gold thickness (nm)	60	59-61	2
Cyclomer thickness (nm)	600	570-630	5
Cyclomer width (nm)	500	400-600	20

The variation between the nominal and the actual values is less than 5% in most cases with the exception of Cyclomer's width. This property has been difficult to control accurately since the 1st Cyclomer run, however, in the latest processing, its deviation from the optimal value has decreased thanks to the UV dose optimization achieved.

5.2 Electrical-Optical characterization

The chips containing the 3rd PLATON mask chip (PLA15W1C2 sample) and the 4x4 switching matrix based on A-MZIs after fabrication was sent to SDU for preliminary characterization. Unfortunately it was observed that coupling light in and out of the chip was very difficult as it requires very careful manual adjustment in 5-axis (x, y, z, θx, θy) of a fiber array. The placement of this fiber arrays was carried out using two microscopes viewing the fiber array and the switching matrix from two perpendicular directions (Figure 5.4). The total measured losses from input to the output of the chip with the current setup is more than 60dB, imposing an insuperable barrier for the characterization of the circuit.

Currently there are efforts for the identification of the high losses of the chip with SEM inspection at UB and simulations by IZM and CERTH. Some factors that are under investigations are the crosspoint between the two stages (see §5.3), the absence of Spin on Glass on top of the Grating Couplers, the coupling efficiency with the fiber array etc. A detailed analysis will be provided with a new version of this deliverable.

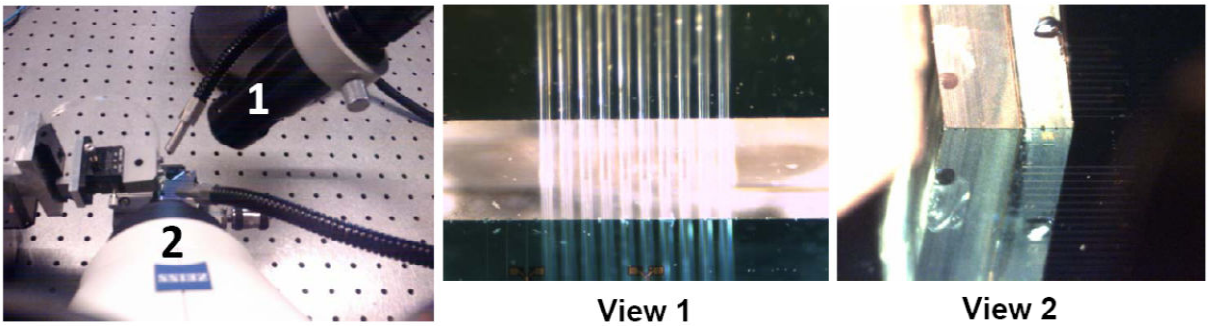

Figure 5.4: Adjustment of coupling with a fiber array using two microscopes viewing the fiber array and a sample from perpendicular directions.

5.3 Characterization of a 4x4 thermooptic Dual Ring Resonator Cyclomer Loaded SPP switching matrix

Cyclomer 4x4 thermally controlled switches relying on dual-racetrack resonator (also known as "X-add-drop") were fabricated by UB and characterized by LRM. The design of this configuration was carried by CERTH after thorough simulations aiming to performance optimization in terms of losses, broadaband operation and extinction ratio at both output ports. More details regarding the design of the X add drop switch can be found in D4.2. The 4x4 thermo-optic DLSPP switching device has also been tested with the fast prototyping process. In this configuration the thermo-electrically control of only one X-add-drop element at a time was not possible due to the gold film that covered completely the surface. Light propagation in this 4x4 switching device has been observed by LRM, as depicted in the following Figure 5.5.

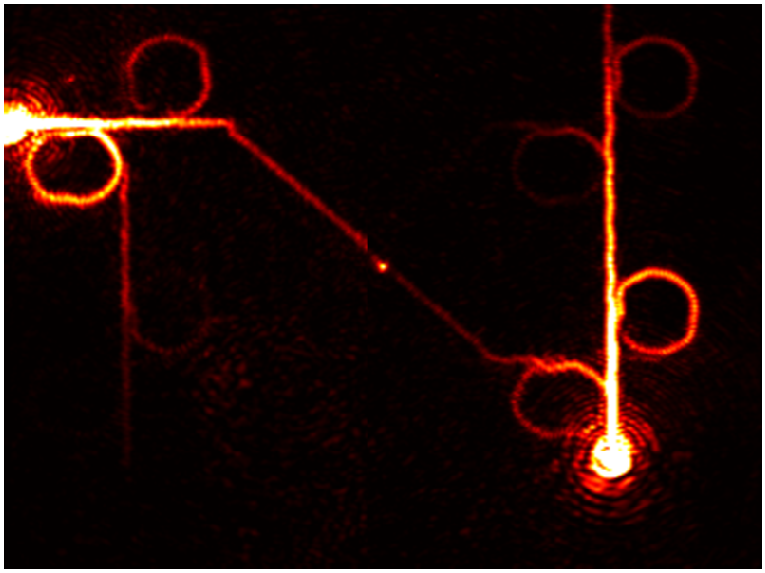

Figure 5.5: Superposition of two leakage radiation microscopy images showing the 4x4 X-add-drop system excited from two different ports.

The first problem observed was a defect spot at the crossing of the two centered waveguides that were used to link each side of the 4x4 system. This defect stemmed directly from the fast prototyping fabrication process. In fact the electron beam exposed the crossing only once, but a second exposure close to the crossing area had to be realized for this switch layout, leading to a local over exposure. This problem will not appear with the usual UV manufacturing process. The second problem concerned the total size of the device that was too large to be characterized with the leakage radiation microscopy used so far. Taking into account that the total size was 2-3 times larger than a single 2x2 switch system, the propagation loss was exponentially increasing and the difference of intensity at the injection compared to the output was too high to be compared, preventing the extraction of a transmission spectrum for each port. An increase in integration time of the infrared camera would allow observing the signal at the output but simultaneously a saturation of the intensity measured at the input would occur.

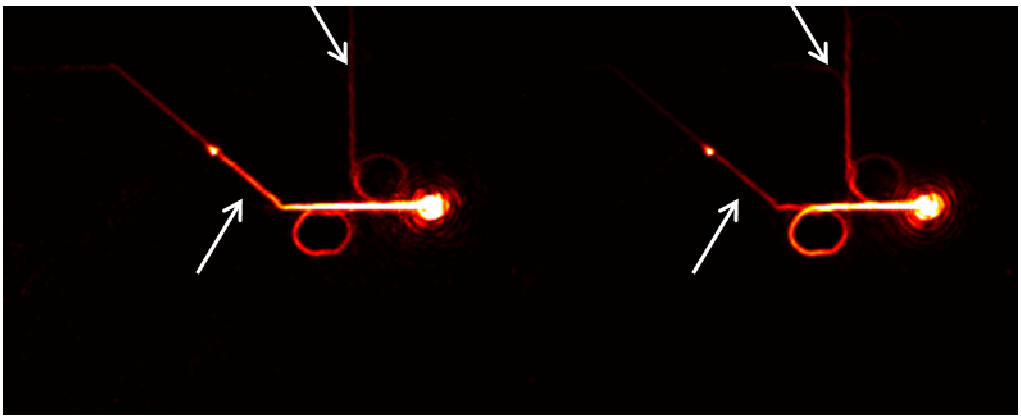

Figure 5.6: 4x4 X-add-drop system made of Cyclomer at two different wavelengths

Finally, the 4x4 system was investigated in terms of correct operation just by sweeping the wavelength. Figure 5.6 represents the same 4x4 system at two different wavelengths (spaced by around 25nm), where the switching of direction between the two ports is clear: On the left image, the signal is mainly directed to the crossing waveguides while on the right image the signal is increased at the upper port and decreased at the cross port. It should be noted that even with the defect at the crossed waveguides section, the signal continued to propagate. This is not expected to be a problem for the UV made structures. The crossing section can also be made of silicon or be improved by special design anticipated by numerical simulations from CERTH.

6 Conclusions

Both normal and asymmetric MZI based 4x4 switching matrices were included in the 3rd PLATON Mask Design and implemented on SOI chips with integrated Si waveguides, by UV lithography and Au lift-off processing. The quality of both the Au and the Cyclomer level components is superior in terms of LER and resolution, with respect to previous chips. This is due to the application of a bi-layer resist process for the gold level fabrication and the optimization of the UV dose factor for the Cyclomer level lithography. The resulting switching elements were characterized structurally by SEM and AFM and their characteristics were found to be consistent to the nominal ones.

The first attempts for complete characterization of the chips were prevented by the difficulty imposed with the usage of fiber arrays for coupling light in and out of the circuits. Despite the arduous efforts carried out by SDU the insertion losses imposed by the chip was >60dB imposing an insuperable barrier for the characterization of the switching matrices. Efforts are under way now for the identification of the losses with SEM characterization of the chip and simulation runs by IZM and CERTH.

Moreover, Cyclomer 4x4 thermally controlled switches relying on dual-racetrack resonators were fabricated by EBL and characterized by Leakage Radiation Microscopy. The 4x4 thermo-optic DLSPP switching device was tested with the fast prototyping process. The switching of direction between the two ports was demonstrated by performing a sweep at a wavelength range of 25nm.

Abbreviations

RLM	Radiation Leakage Microscopy
AFM	Atomic Force Microscope
DLSPP	Dielectric Loaded Surface Plasmon Polariton
DLSPPW	Dielectric Loaded Surface Plasmon Polariton Waveguide
EBL	Electron Beam Lithography
LER	Line Edge Roughness
MZI	Mach Zender Interferometer
RIE	Reactive Ion Etching
SEM	Scanning Electron Microscopy
SOI	Silicon On Insulator